AIAA JOURNAL
Vol. 30, No. 3, March 1992

Multiobjective Shape and Material Optimization of Composite Structures Including Damping

D. A. Saravanos* and C. C. Chamis†
NASA Lewis Research Center, Cleveland, Ohio 44135

A multiobjective optimal design methodology is developed for lightweight, low-cost composite structures of improved dynamic performance. The design objectives may include minimization of damped resonance amplitudes (or maximization of modal damping), weight, and material cost. The design vector includes micromechanics, laminate, and structural shape parameters. Constraints are imposed on static displacements, static and dynamic ply stresses, dynamic amplitudes, and natural frequencies. The effects of composite damping tailoring on the dynamics of the composite structure are incorporated. Applications on a cantilever composite beam and plate illustrate that only the proposed multiobjective formulation, as opposed to single objective functions, may simultaneously improve the objectives. The significance of composite damping in the design of advanced composite structures is also demonstrated, and the results indicate that the minimum-weight design or design methods based on undamped dynamics may fail to improve the dynamic performance near resonances.

Nomenclature

A	= area
$[C],[c]$	= global and modal damping matrices, respectively
E	= normal modulus
$F(z)$	= objective functions
f	= frequency
f_d	= damped frequency
G	= shear modulus
$\boldsymbol{G}(z)$	= inequality constraints
h	= thickness
$[K],[k]$	= global and modal stiffness matrices, respectively
k	= volume ratio
$[M],[m]$	= global and modal mass matrices, respectively
$\boldsymbol{P},\boldsymbol{p}$	= global and modal excitation force, respectively
$\boldsymbol{q}$	= modal vector
S	= strength
t	= time
U	= dynamic amplitude
$\boldsymbol{u}$	= displacement vector
V_f	= average fiber volume per unit area
$\boldsymbol{v}$	= weighting coefficients
$W,\delta W$	= stored and dissipated strain energies
$w,\delta w$	= stored and dissipated specific strain energies, respectively
z	= design vector
θ	= fiber orientation angle
ν	= Poisson's ratio
ρ	= mass density
σ	= stress
$[\Phi]$	= modal matrix
ψ	= specific damping capacity

Subscripts

e	= finite element
f	= fiber
L	= laminate
l	= ply (on axis)
m	= matrix
n	= nth mode

Superscripts

d	= dynamic
L	= lower
s	= static
U	= upper

Direction

1,2,3	= material axes
n	= normal (isotropic material)
s	= shear (isotropic material)
x,y,z	= structural axes

Presented as Paper 90-1135 at the AIAA/ASME/ASCE/AHS/ASC 31st Structures, Structural Dynamics, and Materials Conference, Long Beach, CA, April 2–4, 1990. Received Aug. 17, 1990; revision received March 19, 1991; accepted for publication March 20, 1991.

*Resident Research Associate, Structures Division, 21000 Brookpark Road, Mail Stop 49-8. Member AIAA.

†Senior Research Scientist, Structures Division, 21000 Brookpark Road, Mail Stop 49-8. Member AIAA.

Introduction

FIBER composite materials are widely used in structural applications requiring high stiffness-to-weight and strength-to-weight ratios, as they readily provide high specific moduli, high specific strengths, and tailorable anisotropic elastic properties. A spectrum of design methods has been developed, ranging from basic tailoring of composite laminates to multidisciplinary optimization of composite structures,[1–8] in order to meet requirements for high performance and light weight. However, most design methodologies are primarily based on stiffness and strength tailoring, hence, they can predict good static structural performance, but not necessarily the optimal dynamic performance because they neglect an important dynamic parameter, the passive damping of composite materials.

Polymer-matrix composites are known to exhibit significantly higher damping compared to most common metals. The previously stated requirements for advanced lightweight structures virtually restrict the use of many traditional sources of passive damping, such as discrete dampers and add-on viscoelastic damping layers, therefore, the option to utilize the damping capacity of polymer-matrix composites appears very attractive. Reported research on the damping of unidirectional composites and laminates[9–14] has shown that the damping of composites is highly tailorable and is primarily controlled by constituent parameters (fiber/matrix properties,

fiber volume ratio) and laminate parameters (ply angles/thicknesses, stacking sequence). Additional research work[15] demonstrated that the modal damping of composite structures depends also on the structural geometry and deformation (mode shapes). This work also suggested that properly designed composite structures can provide significant passive damping and they may further improve the dynamic performance and fatigue endurance by attenuating undesirable elastodynamic phenomena such as structural resonances, overshooting, and long settling times. The previous studies have also demonstrated that any increase in damping typically results in decreased stiffness and strength; therefore, any tailoring of the composite material for optimal damped response will be based on tradeoffs between damping, stiffness, and strength.

Although the optimization of composite structures for multiple design criteria including damping appears to be worthwhile and its significance has been acknowledged,[16] reported research on the subject has been mostly limited to the laminate level[17,18] and the optimal tailoring of composite structures for optimal transient or forced dynamic response.[19,20] The latter work, although it was limited to a single objective function and the optimization of fiber orientation angles and fiber volume ratios (FVRs), illustrated that, in order to realize full benefits from the damping capacity of composite materials, integrated methodologies for the optimal design of composite structures should be developed entailing 1) multiple objectives to effectively represent the array of competing design requirements, 2) capability for tailoring the basic composite materials and/or laminate, 3) capability for shape optimization, and 4) design criteria based on the global static and dynamic response of the composite structure.

This paper presents the development of such a formal design method that allows the optimization of composite structures for optimal damped dynamic performance based on multiple objectives. The proposed design objectives are minimization of resonance amplitudes (or maximization of structural damping), minimization of structural weight, and minimization of material cost. The latter objective (material cost) is included because the high material cost has been a critical factor limiting the use of composites. Additional performance constraints are imposed on static deflections, dynamic resonance amplitudes, natural frequencies, static ply stresses, and dynamic ply stresses. The analysis involves unified composite mechanics, which entail micromechanics, laminate, and structural mechanics theories for the passive damping and other mechanical properties of the composite. The structural damping and the damped dynamic response are simulated with finite element analysis. Evaluations of the methodology on the structural optimization of a cantilever composite beam and a cantilever composite plate are presented. The results quantify the importance of structural damping in improving the dynamic performance of composite structures and illustrate the suitability of multiple objectives in the optimal design of composite structures.

Damped Structural Dynamic Response

Assuming that finite element discretization has been applied, the dynamic response of a structure that is excited by a force $\boldsymbol{P}(t)$ is expressed by the following system of dynamic equations:

$$[M]\ddot{\boldsymbol{u}} + [C]\dot{\boldsymbol{u}} + [K]\boldsymbol{u} = \boldsymbol{P}(t) \tag{1}$$

In the case of laminated composite structures, the stiffness, damping, and mass matrices, $[K]$, $[C]$, and $[M]$, respectively, are synthesized utilizing micromechanics, laminate, and structural mechanics theories representing the various material and structural scales in the composite structure.

The related theories for this multilevel simulation of structural composite damping are described in Refs. 9, 10, and 15. Analogous theories are utilized for the synthesis of other mechanical properties.[21] At the micromechanics level, the on-axis damping capacities of the basic composite material systems are calculated based on constituent properties, material microstructure, FVR, temperature, and moisture. The off-axis damping capacities of the composite plies are calculated at the laminate level, and the local laminate damping matrices are predicted based on on-axis damping values, ply thicknesses, and laminate configuration. The damping contributions of the interlaminar matrix layers due to in-plane interlaminar shear are also incorporated. The interlaminar layer damping was found to be significant for angle-ply laminates.[10]

The structural modal damping is synthesized by integrating the local damping contributions over the structural volume. The modal specific damping capacity (SDC) of the nth vibration mode ψ_n is

$$\psi_n = \frac{\int_A \delta W_{Ln}\, dA}{\int_A W_{Ln}\, dA} \tag{2}$$

where δW_{Ln} and W_{Ln} are the dissipated and maximum stored laminate strain energy distributions, respectively, of the nth mode per unit area per cycle. Utilizing the finite element discretization scheme proposed in Ref. 15, the modal SDC is related to the element damping and stiffness matrices, $[C_e]$ and $[K_e]$, respectively,

$$\psi_n = \frac{\frac{1}{2}\sum_{i=1}^{\text{nel}} \boldsymbol{u}_{ein}^T [C_{ei}] \boldsymbol{u}_{ein}}{\frac{1}{2}\sum_{i=1}^{\text{nel}} \boldsymbol{u}_{ein}^T [K_{ei}] \boldsymbol{u}_{ein}} \tag{3}$$

where nel is the total number of elements and $\boldsymbol{u}_{ein}$ the nodal displacements of the ith element corresponding to the nth vibration mode.

The dynamic response of the structure is simulated based on modal superposition. The dynamic system in Eq. (1) is transferred to the $p \times p$ modal space via the linear transformation $\boldsymbol{u} = [\Phi]\boldsymbol{q}$. Assuming proportional damping and utilizing the first p modes, the following set of p uncoupled dynamic equations results:

$$[m]\ddot{\boldsymbol{q}} + [c]\dot{\boldsymbol{q}} + [k]\boldsymbol{q} = \boldsymbol{p}(t) \tag{4}$$

The frequency response of the structure would be

$$\boldsymbol{u}(f) = [\Phi]\boldsymbol{q}(f) \tag{5}$$

where $\boldsymbol{q}(f)$ is the frequency response in the modal space induced by a harmonic force $\boldsymbol{P}\sin(2\pi ft)$ of frequency f. A typical

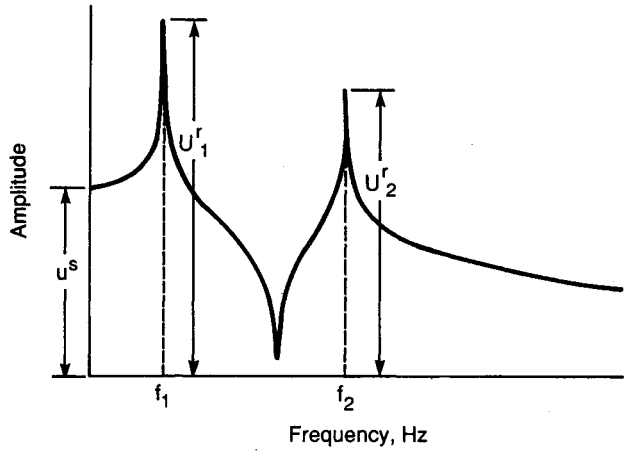

Fig. 1 Typical frequency response function.

frequency response function (FRF) is shown in Fig. 1. The dynamic amplitude U_j^d at a frequency f is the complex magnitude of the displacement $u_j(f)$,

$$U_j^d(f) = |u_j(f)| \tag{6}$$

The resonance amplitude U_{jn}^d at the nth vibration mode is

$$U_{jn}^d = |u_j(f_{dn})| \tag{7}$$

where f_{dn} is the nth damped natural frequency. The dynamic and resonance amplitudes in Eqs. (6) and (7) are used as dynamic performance measures. The resonance amplitudes are primarily related to modal damping and they decrease as the damping increases. Increased modal stiffness will also reduce the respective resonance amplitudes.

Multiobjective Optimal Design

As previously explained, damping is one of the factors that controls the dynamic performance of composite structures near resonances. High damping values result in improved vibration control and fatigue endurance. Proposed design methods for optimizing the undamped dynamic performance of composite structures will fail to utilize the full potential of composite materials and may increase the dynamic amplitudes near resonances.

The design of composite structures for optimal dynamic performance is a multiobjective task and may be best accomplished as the constrained minimization of multiple objective functions. Increases in composite damping may typically result in stiffness/strength reduction and/or mass addition; for this reason, the minimization of weight and material cost is also included in the objectives. The material cost is a crucial factor, restricting in many cases the use of composite materials. Moreover, the distinction between weight minimization and material cost minimization is also stressed because fiber-reinforced composites are nonhomogeneous materials and the minimization of the weight does not also imply the minimization of the material cost.

A constrained multiobjective problem involving minimization of l objective functions is described in the following mathematical form:

$$\min\{F_1(z), F_2(z), \ldots, F_l(z)\} \tag{8}$$

subject to lower and upper bounds on the design vector z and inequality constraints $G(z)$:

$$z^L \le z \le z^U \tag{9}$$

$$G(z) \le 0 \tag{10}$$

In the rest of the paper, upper and lower values are represented by superscripts U and L, respectively. Individual minimizations of each objective function subject to constraints (9) and (10) will result in a set of l ideal solutions $\boldsymbol{F}_1 = (F_1^*, F_2, \ldots, F_l)$, $\boldsymbol{F}_2 = (F_1, F_2^*, \ldots, F_l)$, and so forth. These ideal solutions define a target point $\boldsymbol{F}^* = (F_1^*, F_2^*, \ldots, F_l^*)$ in the objective function subspace, which usually lies in the infeasible domain. Hence, a candidate solution may be obtained by finding a feasible point $\boldsymbol{F} = (F_1, \ldots, F_l)$ in the objective function subspace as closely as possible to the target point $\boldsymbol{F}^*$. This is equivalent to minimizing the distance between points $\boldsymbol{F}$ and $\boldsymbol{F}^*$ subject to constraints (9) and (10), that is,

$$\min\|\boldsymbol{F} - \boldsymbol{F}^*\| \tag{11}$$

where the symbol $\| \ \|$ implies an admissible metric. In the present study, a weighted Euclidean metric is chosen for its simplicity and physical meaning. Scaling is typically required to overcome the problem of different physical quantities represented by the various objective functions. Hence, the original multiobjective problem becomes a constrained minimization of the following scaled objective function:

$$\min \sum_{i=1}^{l} v_i \frac{(F_i - F_i^*)^2}{F_i^{*2}} \tag{12}$$

subject to constraints (9) and (10). The weighting coefficients are represented with v_i. Other metrics or scaling procedures may be utilized in Eq. (12), but in general, they are expected to result in different solutions.

In the present method, the design objectives include minimization of 1) the maximum resonance amplitude ($F_1 = \max\{U_{jn}^d\}$), 2) the total structural weight $W(F_2 = W)$, and 3) the material cost represented by the average cost of fibers $P_f(F_3 = P_f)$. The resonance amplitudes are related to modal stiffness, modal damping, and modal mass; hence, the proposed objective function F_1 will tune the modal stiffness, damping, and mass. Alternatively, F_1 may represent modal damping values. The explicit maximization of modal damping may be preferred in the case of a priori unknown dynamic excitations. The use of fiber cost as a measure of the total material cost is justified in view of the very high cost of fibers compared to the cost of matrix. The design vector includes FVRs, ply angles, and shape parameters. The proposed design criteria are then formulated in the following form:

$$\min\{F_1, F_2, F_3\} \tag{13}$$

subject to explicit constraints (9), constraints on the static deflections $\boldsymbol{u}_s$,

$$\boldsymbol{u}^s \le \boldsymbol{u}^{sU} \tag{14}$$

dynamic amplitudes (including dynamic resonance amplitudes),

$$\boldsymbol{U}^d(f) \le \boldsymbol{U}^{dU} \tag{15}$$

$$\boldsymbol{U}_n^d \le \boldsymbol{U}_n^{dU} \tag{16}$$

and natural frequencies $\boldsymbol{f}_n$,

$$\boldsymbol{f}^L \le \boldsymbol{f}_n \le \boldsymbol{f}^U \tag{17}$$

Static failure constraints are imposed on the static ply stresses $\{\sigma_{fl}^s\}$ in the form of the modified distortion energy criterion[21]:

$$\left(\frac{\sigma_{f11}^s}{S_{f11}^s}\right)^2 + \left(\frac{\sigma_{f22}^s}{S_{f22}^s}\right)^2 + \left(\frac{\sigma_{f12}^s}{S_{f12}^s}\right)^2 - \kappa_{f12}\frac{\sigma_{f11}^s}{S_{f11}^s}\frac{\sigma_{f22}^s}{S_{f22}^s} - 1 \le 0 \tag{18}$$

Additional dynamic (fatigue) failure constraints are imposed on the dynamic ply stresses $\{\sigma_{fl}^d(f)\}$ for various frequency values, including the resonance frequencies, to ensure sufficient fatigue endurance:

$$\left(\frac{\sigma_{f11}^d}{S_{f11}^d}\right)^2 + \left(\frac{\sigma_{f22}^d}{S_{f22}^d}\right)^2 + \left(\frac{\sigma_{f12}^d}{S_{f12}^d}\right)^2 - \kappa_{f12}\frac{\sigma_{f11}^d}{S_{f11}^d}\frac{\sigma_{f22}^d}{S_{f22}^d} - 1 \le 0 \tag{19}$$

The ply stresses are calculated from the discretized generalized element stress field. The theoretical background for the calculation of the static/dynamic ply stresses from the generalized element stresses, and the calculation of respective static/dynamic ply strengths $S_{f11}, S_{f22}, S_{f12}$ is provided in Refs. 21 and 22. The biaxial coefficient κ_{f12} is related to the normal moduli, Poisson's ratios, and, optionally, to experimental correlations. It is recalled that the ply strengths are related to constituent properties, fiber volume ratio, and environmental (hygrothermal) effects. The dynamic strengths are also related to the desirable service life of the component.

This constrained optimization problem is solved with the modified feasible directions nonlinear programming method.[23]

Applications and Results

The proposed design method was applied on the optimal tailoring of a cantilever graphite/epoxy composite beam (case 1) and a cantilever graphite/epoxy composite plate (case 2). The initial beam shape, 152.4 mm (6 in.) long, 25.4 mm (1 in.) wide, and 5.08 mm (0.2 in.) thick, is shown in Fig. 2a. The initial plate geometry, 406.4 mm (16 in.) long, 406.4 mm (16 in.) wide, and 5.08 mm (0.2 in.) thick, is shown in Fig. 2b. A unidirectional ply configuration was selected as the initial reference design for both cases because it provides the higher axial bending rigidity. Typical properties of the composite material in room conditions are shown in Table 1. Both structures were assumed to operate in room conditions. The SDCs of the fibers and matrix were back calculated from the respective SDCs of the unidirectional composite reported in Ref. 12. The laminate configuration in both structures is symmetric, consisting of angle-ply sublaminates 1, 2, and 3 in each side. All sublaminates have plies of equal thickness [0.254 mm (0.01 in.)]. Sublaminate 3 is at the center of the laminate as illustrated in Fig. 2c, where the laminate configuration $[(\pm\theta_1)_2/(\pm\theta_2)_2/(\pm\theta_3)]_s$ for the initial uniform thickness is shown. The ply angles θ_i and FVRs k_{fi} of each sublaminate and the thicknesses h_j at 0, 30, 60, and 100% (tip) of the span were the design variables. The thickness at other sections was interpolated using a cubic spline fit. It was further assumed that, when the thickness of a cross section was reduced, the inner ply of sublaminate 3 would first reduce in thickness and eventually drop. The remaining plies of sublaminate 3 will follow, and if necessary, the inner plies of sublaminates 2 and 1 would drop subsequently. In the opposite case of increased thickness, inner plies of maximum 0.254 mm (0.01 in.) thickness are added to sublaminate 1. Considering the scope of the present paper, this seems to be a reasonable approximation, but in future work, discrete ply drops in connection with discrete optimization techniques may be also investigated. Because the same fibers were used in all sublaminates, the material cost was measured as the total fiber volume in the structure $V_f(F_3 = V_f)$. The weighting coefficients in Eq. (12) were set equal to unity. The following upper and lower bounds were imposed on the design variables:

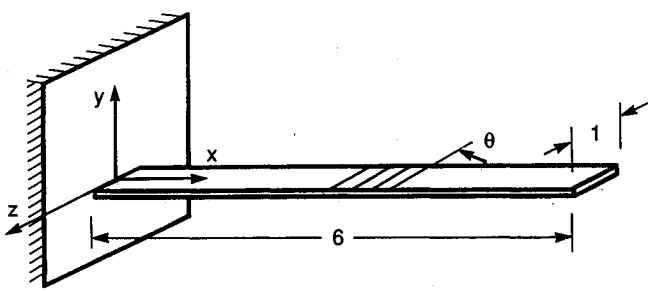

a)

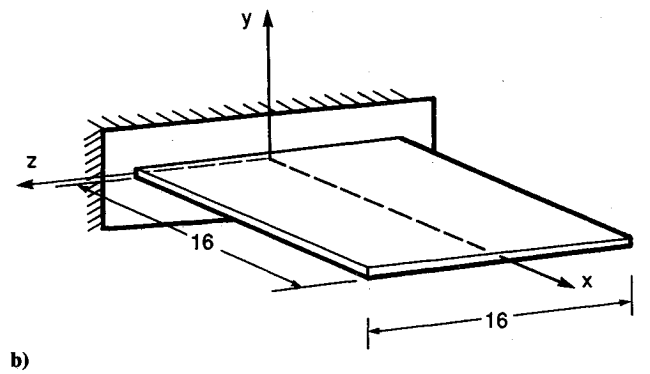

b)

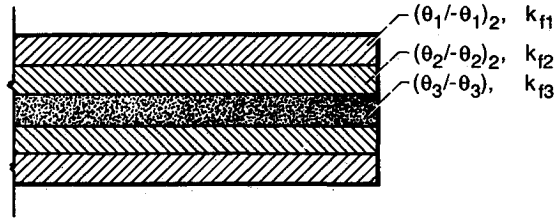

c)

Fig. 2 Candidate composite structures: a) initial beam geometry; b) initial plate geometry; c) laminate configuration (dimensions are in inches; 1 in. = 25.4 mm).

$$-90.0 \text{ deg} \le \theta_i \le 90.0 \text{ deg} \tag{20}$$

$$0.01 \le k_{fi} \le 0.70 \tag{21}$$

$$1.016 \text{ mm } (0.04 \text{ in.}) \le h_j \le 10.16 \text{ mm } (0.4 \text{ in.}) \tag{22}$$

In both cases, the weight and material cost increases were restricted to be <15% of the respective values of the reference design. The calculation of dynamic strengths in constraints (19) was based on a minimal fatigue life of 10^4 cycles. The dynamic stress constraints were imposed at each of the first four resonance frequencies for the respective harmonic loads applied in each case.

Case 1: Composite Beam

A finite element mesh of 55 nodes and 80 specialty triangular plate elements[15] was utilized. A static transverse out-of-plane (y-axis) force of 8760 N/m (50 lb/in.) and a transverse out-of-plane harmonic force of 17.5 N/m (0.1 lb/in.) amplitude were applied at the tip of the beam. Under this type of dynamic loading, the maximum resonance amplitude at the tip corresponds to the first mode (first out-of-plane bending) $(F_1 = U^d_{y1})$. In addition to constraints (18–22), constraints included upper bounds on the transverse static deflections at the free end,

$$u^s_y \le 8.89 \text{ mm } (0.35 \text{ in.}) \tag{23}$$

lower bounds on the first two natural frequencies,

$$f_1 \ge 400 \text{ Hz}, \qquad f_2 \ge 1200 \text{ Hz} \tag{24}$$

and upper bounds on the transverse resonance amplitudes at the tip, for each of the first four modes:

$$U^d_{yn} \le 11.43 \text{ mm } (0.45 \text{ in.}), \qquad n = 1, \ldots, 4 \tag{25}$$

Table 2 shows the initial reference design, the three single-objective optimal designs (each objective function individually optimized), and the resultant multiobjective optimal design. The predicted resonance amplitudes at the tip, natural frequencies, and modal specific damping capacities of the first

Table 1 Mechanical properties of HM-S/epoxy system (70°F and 0% moisture)

Epoxy	HM-S graphite
$E_m = 0.500$ Mpsi (3.45 GPa)	$E_{f11} = 55.0$ Mpsi (379.3 GPa)
$G_m = 0.185$ Mpsi (1.27 GPa)	$E_{f22} = 0.9$ Mpsi (6.2 GPa)
$\psi_{mn} = 10.30\%$	$G_{f12} = 1.1$ Mpsi (7.6 GPa)
$\psi_{ms} = 11.75\%$	$\nu_{f12} = 0.20$
$\rho_m = 0.0440$ lb/in.^{3} (1.218 g/cm^3)	$\psi_{f11} = 0.4\%$
	$\psi_{f22} = 0.4\%$
	$\psi_{f12} = 0.4\%$
	$\rho_m = 0.0703$ lb/in.^{3} (1.946 g/cm^3)

Table 2 Initial and optimum designs of the composite beam (case 1)

	Initial design	Single-objective designs			Multiobjective design
		min F_1	min F_2	min F_3	
Thickness, mm					
0% span	5.08	6.32	5.41	5.65	5.88
30% span	5.08	6.25	4.76	5.61	5.85
60% span	5.08	6.55	3.66	5.68	5.69
100% span	5.08	3.75	1.02	1.02	1.02
Ply angles, deg					
θ_1	0.0	24.68	13.55	4.306	24.46
θ_2	0.0	24.05	−41.19	41.150	53.53
θ_3	0.0	−50.33	−65.56	44.863	90.00
Fiber volume ratios					
k_{f1}	0.50	0.637	0.630	0.294	0.512
k_{f2}	0.50	0.700	0.021	0.010	0.010
k_{f3}	0.50	0.010	0.010	0.010	0.010
Objective functions					
F_1 (mm)	10.10	3.09	11.14	11.21	5.17
F_2 (g)	30.71	35.38	21.05	24.40	26.08
F_3 (cm^3)	9.83	10.48	4.88	2.37	4.04
Natural frequencies, Hz					
f_1	387.4	424.2	504.9	400.0	400.0
f_2	1095.3	1457.9	1936.2	1254.3	1362.5
f_3	1549.7	2476.7	2025.5	1340.1	2078.0
Resonance y-axis amplitudes (tip), mm					
U^d_{y1}	10.10	3.10	11.15	11.30	5.21
U^d_{y2}	0.00	0.00	0.00	0.00	0.00
U^d_{y3}	0.00	0.10	0.46	0.00	0.02
Modal SDCs, %					
ψ_1	0.604	1.679	0.831	0.880	1.941
ψ_2	5.592	3.202	1.490	2.677	2.742
ψ_3	3.503	2.021	1.334	5.543	2.288

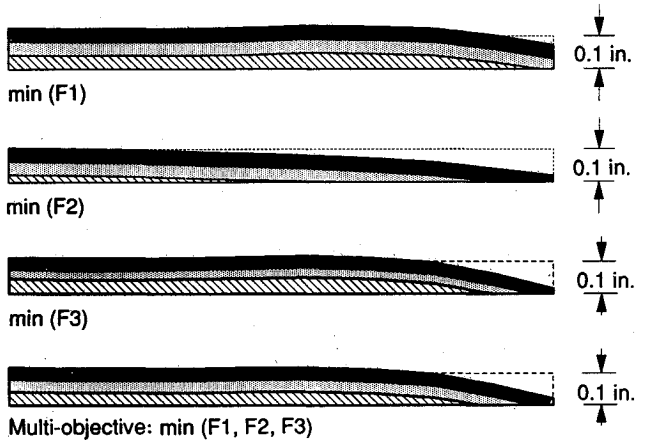

Fig. 3 Optimum half-thickness distributions of the composite beam, case 1 (1 in. = 25.4 mm).

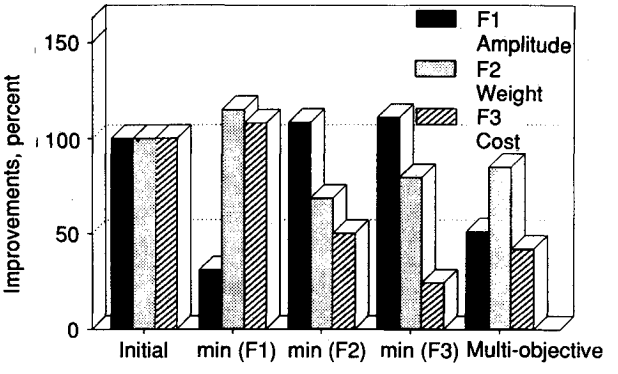

Fig. 4 Relative changes in the objective functions, case 1.

3 modes are also shown. As seen in Table 2, the initial design violates both frequency constraints, but all optimized designs have natural frequencies in the feasible frequency domain. All optimized designs have nonuniform thickness, being thicker at the proximal end and thinner at the distal end. Side views of the optimized thickness shapes for each optimization case are plotted in Fig. 3. The apparent differences among the optimal shapes demonstrate the significance of shape optimization. The relative improvements of each objective function with respect to the reference design are plotted in Fig. 4.

The minimization of the resonance tip amplitude (minF_1) decreased the resonance peak by 69% with respect to the unidirectional beam. This reduction was attained by a combination of high modal stiffness and damping. The optimization resulted in increased weight (15%), increased material cost (8%), and redistribution of the material. The near ∓24-deg ply angles in the two outer sublaminates contribute to high flexural damping and increased in-plane shear stiffness, whereas the high FVRs provide out-of-plane flexural stiffness. The inner ply was virtually reduced to pure matrix and primarily contributes to damping. Active constraints at the optimum were the upper bounds on weight and cost and the first natural frequency constraint.

The minimum weight design (minF_2) decreased the weight of the beam by 31% and the material cost by 50%, but increased the resonance amplitude by 8% with respect to the initial design. The weight reduction was primarily accomplished by material redistribution and lower FVRs in all sublaminates (the fibers have higher density than the matrix). The lower ply angles in the outer sublaminate also contributed to the weight reduction because they provided high specific flexural rigidity and strength. Both inner sublaminates were virtually reduced to pure matrix, resulting in a sandwich-type laminate configuration. The first modal damping has moderately increased. Active constraints at the optimum were static and dynamic displacement constraints and static stress constraints.

The minimum cost design (minF_3) decreased the material cost by 76% and the structural weight by 20%, but increased

the first resonance amplitude by 11%. Interestingly, the ply angles of the outer sublaminate are ±4.3 deg, an almost unidirectional configuration. The FVRs of all sublaminates were reduced to pure matrix. This type of laminate tailoring requires the least amount of fibers; hence, it provides the ultimate utilization of the reinforcing fibers. The first modal damping of the optimized beam was low. The frequency constraints, static and dynamic amplitude constraints, and dynamic stress constraints were active at the optimum.

As shown in Fig. 4, all individual minimizations of each objective function failed to produce simultaneous improvements in all objectives. In contrast, the resultant multiobjective optimal design seems to blend many merits of the individual single-objective optimizations since all objective functions were significantly reduced compared to the initial design. Specifically, the first resonance amplitude was decreased by 49%, the structural weight by 15%, and the material cost by 58%. This clearly illustrates the superiority and suitability of the multiobjective optimal design for beamlike composite structural components. The optimum laminate configuration is composed of an outer ±24-deg angle-ply sublaminate of 51% FVR providing all stiffness and strength and two inner sublaminates of virtually pure matrix. The present optimal design exhibits the higher value of the first modal SDC than all other designs, which demonstrates the importance of damping tailoring in connection to the multiple objectives. The first natural frequency constraint and static deflection constraints were active at the optimum.

The frequency response functions at the midpoint of the free edge of the initial and optimized beams are shown in Fig. 5. As was expected, the multiobjective optimum design has a better FRF than the minimum cost and minimum weight designs. This suggests that the incorporation of composite damping was crucial in obtaining these significant improvements in all objective functions illustrating, in this manner, the significance of composite damping in the design of high dynamic performance, lightweight, and low-cost composite structures.

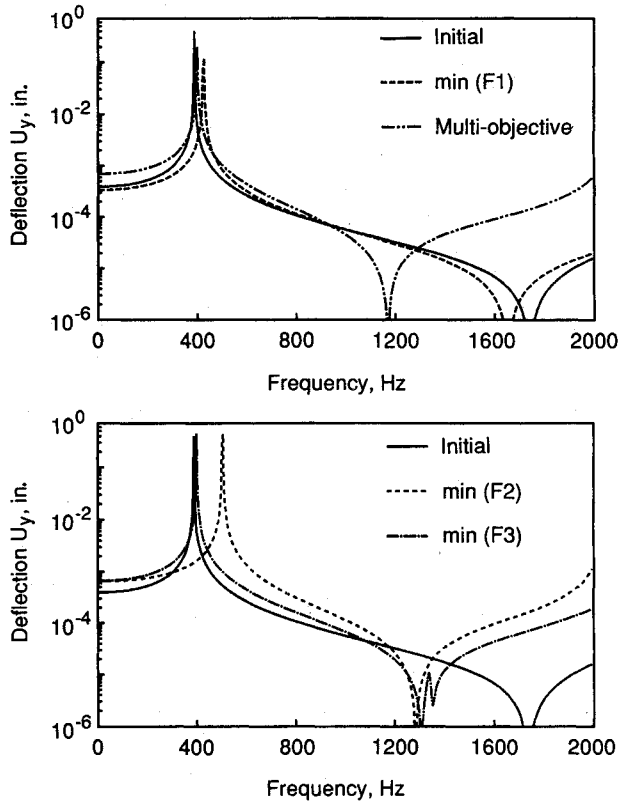

Fig. 5 Frequency response functions of the initial and optimal designs of the composite beam, case 1 (1 in. = 25.4 mm).

Case 2: Composite Plate

A finite element mesh of 45 nodes and 65 triangular plate elements[15] was used to model the plate. A uniform static transverse out-of-plane (y-axis) force of 546.6 N/m (3.12 lb/in.) was applied at the free end. An additional combination of dynamic loads consisting of a uniform transverse out-of-plane harmonic force of 1.104 N/m (0.0063 lb/in.) (amplitude) and a twisting harmonic moment of 0.139 N-m/m (0.0313 lb-in./in.) (amplitude) were applied at the free edge of the plate. Under this type of dynamic loading, the maximum resonance amplitude at the tip typically occurs either at the first mode (first out-of-plane bending for the initial design) or at the second mode (first torsion for the initial design). In addition to constraints (18–22), constraints included upper bounds on the transverse static deflections of the free end,

$$u_y^s \leq 12.70 \text{ mm } (0.50 \text{ in.}) \tag{26}$$

lower bounds on the first four natural frequencies,

$$f_1, f_2 \geq 50 \text{ Hz}, \qquad f_3, f_4 \geq 200 \text{ Hz} \tag{27}$$

and upper bounds on the transverse resonance amplitudes of the free end for the first four modes:

$$U_{yn}^d \leq 11.45 \text{ mm } (0.45 \text{ in.}), \qquad n = 1,\ldots,4 \tag{28}$$

Table 3 shows the initial reference design, the three single-objective optimal designs, and the resultant multiobjective optimal design. Table 3 also shows the dynamic characteristics of each design, such as resonant frequencies, maximum dynamic deflections in the y direction at the free edge for each mode, and modal SDCs. The resultant optimum thickness distributions are shown in Fig. 6, and the relative changes in the objective function values with respect to the initial unidirectional plate are shown in Fig. 7. Although the initial design violates three frequency constraints, the optimal designs satisfied all constraints. The observed tendency of the optimum designs in case 1 (beam) to result in composite sandwich laminate configurations with a constrained matrix layer in the middle was more predominant in the present case, as all optimum designs reduced in composite plates with thick matrix cores (sublaminates 2, 3) and angle-ply composite skins (sublaminate 1) that provide stiffness and strength. Apparently, this is the best configuration for combinations of high stiffness, strength, damping (constrained damping layer), and low material cost. This interesting result was the direct benefit of introducing unified micromechanics into the analysis and, consequently, the FVRs into the design parameters. The optimal designs differ drastically in optimal thickness shapes (Fig. 6), ply angles, FVRs, objective function values, and dynamic characteristics, which demonstrates the inherent tendency of composite structures to get overdesigned.

The minimization of the resonance amplitude ($\min F_1$) decreased drastically the amplitudes of modes 1 (66%) and 2. In fact, it resulted in almost equal maximum resonant amplitudes for the first two modes. The material cost (total fiber volume) was also reduced, but the weight increased to the upper limit. Sublaminates 2 and 3 were reduced to matrix, and sublaminate 1 has ± 11.7-deg angle plies and very high FVR. The modal SDCs have intermediate values, indicating that the reductions in the resonant amplitudes were obtained by tuning the respective modal stiffness, mass, and damping values. The constraints on the third natural frequency and the structural weight were active at the optimum.

The minimum weight design ($\min F_2$) resulted in reduced weight (15%) and reduced cost (45%), but increased the first resonant amplitudes to the upper bound. The outer sublaminate has again very high FVR and ± 25-deg angle plies. Similarly, with case 1 (beam), the minimum weight design resulted in high resonant amplitudes and very low modal

Table 3 Initial and optimum designs of the composite beam (case 2)

	Initial design	Single-objective designs			Multiobjective design
		min F_1	min F_2	min F_3	
Thickness, mm					
0% span	5.08	10.12	7.10	9.88	10.16
30% span	5.08	9.30	6.35	7.89	8.06
60% span	5.08	6.18	4.45	8.48	8.19
100% span	5.08	1.02	1.02	1.02	1.02
Ply angles, deg					
θ_1	0.0	11.74	24.91	33.97	24.23
θ_2	0.0	−83.10	50.38	68.88	49.92
θ_3	0.0	−4.06	56.22	−47.84	−52.70
Fiber volume ratios					
k_{f1}	0.50	0.700	0.698	0.225	0.301
k_{f2}	0.50	0.010	0.010	0.010	0.010
k_{f3}	0.50	0.010	0.010	0.010	0.010
Objective functions					
F_1 (mm)	9.88	3.35	11.43	5.81	5.18
F_2 (g)	1311.8	1508.6	1114.0	1508.6	1508.6
F_3 (cm^3)	414.6	237.0	229.4	83.1	108.1
Natural frequencies, Hz					
f_1	41.6	117.0	81.1	50.0	66.1
f_2	46.5	133.1	123.4	111.5	114.6
f_3	200.0	200.0	200.0	200.0	200.0
f_4	251.2	383.8	303.8	276.2	341.9
Maximum resonance y-axis amplitudes (tip), mm					
U^d_{y1}	9.88	3.35	11.43	5.82	5.18
U^d_{y2}	5.23	3.15	8.31	2.03	2.26
U^d_{y3}	0.28	0.30	0.46	1.24	0.02
U^d_{y4}	0.30	1.07	0.91	0.61	0.46
Modal SDCs, %					
ψ_1	1.327	1.028	0.690	2.000	1.300
ψ_2	3.181	1.604	0.756	1.550	1.497
ψ_3	3.327	1.870	0.947	2.636	2.349
ψ_4	1.556	1.107	0.742	1.909	1.494

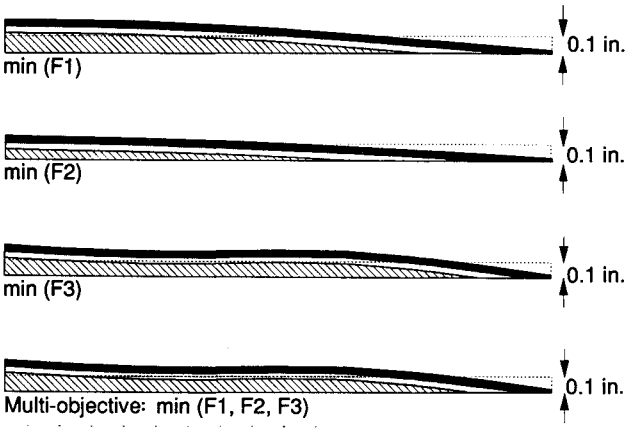

Fig. 6 Optimum half-thickness distributions of the composite plate, case 2 (1 in. = 25.4 mm).

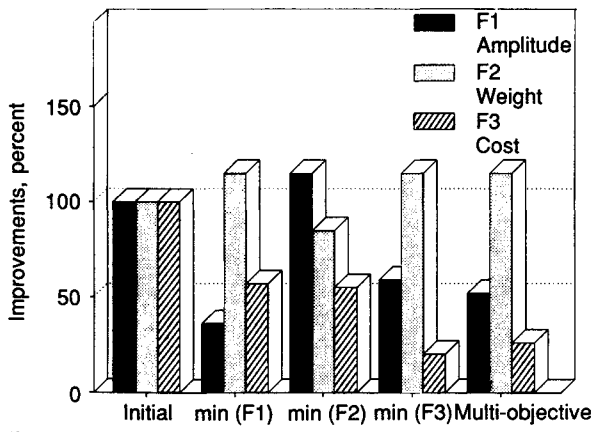

Fig. 7 Relative changes in the objective functions, case 2.

damping values, which demonstrates the unsuitability of the minimum weight formulation for improving the dynamic performance of composite structures. Active at the optimum were the constraint on the third natural frequency and constraints on the dynamic amplitudes.

The minimum cost design resulted in significantly reduced material cost (80%), reduced resonant amplitudes, and increased weight (15%). The FVR of the outer sublaminate is low. The high modal damping of the first mode and the resultant thickness shape shown in Fig. 5, with an apparent mass concentration near the three quarters of the span, indicate that both modal damping and mass distribution were critical in satisfying the performance requirements. The first and third natural frequency constraints and the upper bound on the weight were active at the optimum.

The multiobjective design blends attributes of the minimum amplitude and minimum cost designs. The weight increased because of its insensitivity compared to the other objective functions; that is, the 15% tradeoff in weight was outnumbered by high reductions in the maximum resonant amplitudes (48%) and material cost (74%). The outer sublaminate has ±24-deg angle plies of intermediate FVR. The first modal damping is high, illustrating the importance of damping in the reduction of the respective resonant amplitude. The constraints on the third natural frequency and the weight were active.

The resultant frequency response functions of the transverse y-axis deflection at the foremost corner of the plate (x = 16 in., z = 8 in.), where the maximum dynamic deflection was observed for almost all optimal designs, are plotted in Fig. 8. The multiobjective, the minimum amplitude, and the minimum cost designs have improved FRFs compared to both initial and minimum weight designs. Interestingly, the minimum weight design has the higher resonance amplitudes, even than the initial plate, illustrating once more the unsuitability of the minimum weight design for improving the dynamic performance. As both case studies illustrated, optimal

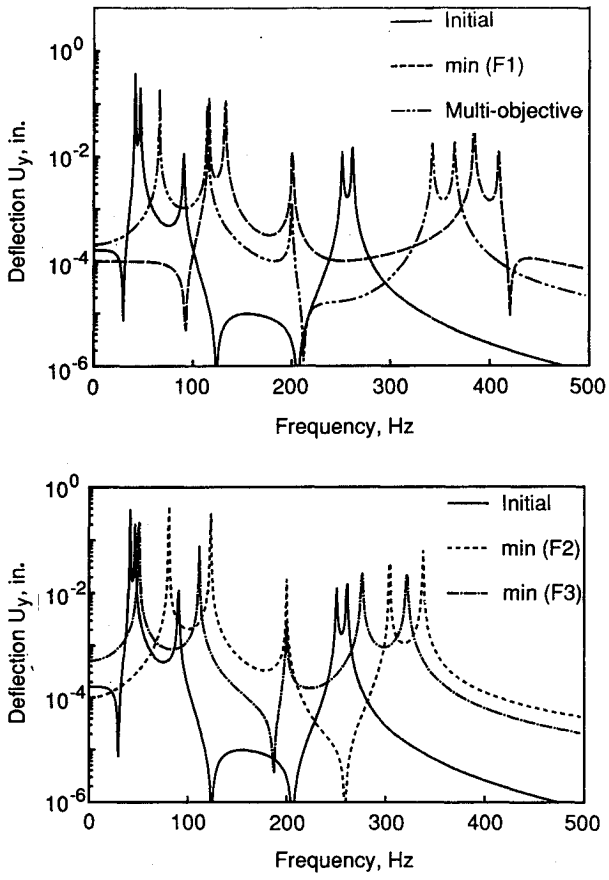

Fig. 8 Frequency response functions of the initial and optimal designs of the composite plate, case 2 (1 in. = 25.4 mm).

design methodologies neglecting the damping capacity of composite materials and its controllable anisotropy may lead to structures with inferior dynamic performance near the resonance regimes; hence, they appear unsuitable for optimizing the dynamic performance of composite structures.

Summary

An optimal design methodology for optimizing the dynamic performance of composite structures based on multiple objectives was proposed. The design objectives included minimization of resonance amplitudes, minimization of structural weight, and minimization of material cost. The effects of composite passive damping on the dynamic response of composite structures were incorporated into the analysis via integrated micromechanics, laminate mechanics, and structural mechanics theories. Performance constraints were imposed on static displacements, static stresses, dynamic resonance amplitudes, natural frequencies, and dynamic stresses. The described method has been integrated into an in-house research code.[8]

The method was applied on the optimal design of a cantilever composite beam and a cantilever plate. In both cases, the multiobjective optimization was proved superior in minimizing the competing requirements for high damping, low weight, and low material cost and resulted in significant simultaneous improvements in the objective functions. The resultant optimal designs illustrated that both material (fiber orientation angles, fiber volume ratios) and shape parameters contributed to the obtained improvements. The unique inclusion of damping micromechanics into the analysis and the incorporation of fiber volume ratios in the method resulted in sandwich-type optimum laminate configurations consisting of a matrix core and a composite skin. This type of laminate resembles the constrained configuration damping layer and seems to provide the desirable combinations of high specific stiffness, strength, and damping.

The optimizations with single-objective functions have shown a strong tendency to overdesign the structure and did not improve all objectives. The obtained results for both structures (beam and plate) illustrated that the damping capacity of composites is an important factor in designing lightweight, low-cost composite structures of improved dynamic performance. It was further shown that the traditional minimum-weight design, or other proposed methods for optimizing the undamped dynamic response of composite structures, may fail to improve or may even deteriorate the dynamic performance near resonance because they neglect the tailorable damping capacity of composite materials. Overall, the applications of the method appeared very encouraging. Additional studies on more complex structural configurations and dynamic excitations may well be worth the effort; therefore, they are recommended as future research topics.

References

[1]Schmit, L. A., and Farhsi, B., "Optimum Design of Laminated Fibre Composite Plates," *International Journal for Numerical Methods in Engineering*, Vol. 11, No. 4, 1977, pp. 623–640.

[2]Schmit, L. A., and Mehrinfar, M., "Multilevel Optimum Design of Structures with Fiber-Composite Stiffened-Panel Components," *AIAA Journal*, Vol. 20, No. 1, 1982, pp. 138–147.

[3]Tauchert, T. R., and Adibhatla, S., "Design of Laminated Plates for Maximum Stiffness," *Journal of Composite Materials*, Vol. 18, No. 1, 1984, pp. 58–69.

[4]Adali, S., "Multiobjective Design of an Antisymmetric Angle-Ply Laminate by Nonlinear Programming," *Journal of Mechanisms, Transmissions, and Automation in Design*, Vol. 105, No. 2, 1983, pp. 214–219.

[5]Hajela, P., and Shih, C. J., "Optimal Design of Laminated Composites Using a Modified Mixed Integer and Discrete Programming Algorithm," *Computers and Structures*, Vol. 32, No. 1, 1989, pp. 213–221.

[6]Vanderplaats, G. N., and Weisshaar, T. A., "Optimum Design of Composite Structures," *International Journal for Numerical Methods in Engineering*, Vol. 27, No. 2, 1989, pp. 437–448.

[7]Haftka, R. T. et al., "Efficient Optimization of Integrated Aerodynamic-Structural Design," *International Journal for Numerical Methods in Engineering*, Vol. 28, No. 3, 1989, pp. 593–607.

[8]Brown, K. W., "Structural Tailoring of Advanced Turboprops (STAT)—Interim Report," NASA CR-180861, Aug. 1988.

[9]Saravanos, D. A., and Chamis, C. C., "Unified Micromechanics of Damping for Unidirectional and Off-Axis Fiber Composites," *Journal of Composites Technology and Research*, Vol. 12, No. 1, 1990, pp. 31–40.

[10]Saravanos, D. A., and Chamis, C. C., "Mechanics of Damping for Fiber Composite Laminates Including Hygro-Thermal Effects," *AIAA Journal*, Vol. 28, No. 10, 1990, pp. 1813–1819.

[11]Adams, R. D., and Bacon, D. G. C., "Effect of Fibre Orientation and Laminate Geometry on the Dynamic Properties of CFRP," *Journal of Composite Materials*, Vol. 7, No. 4, 1973, pp. 402–428.

[12]Ni, R. G., and Adams, R. D., "The Damping and Dynamic Moduli of Symmetric Laminated Composite Beams—Theoretical and Experimental Results," *Journal of Composite Materials*, Vol. 18, No. 2, 1984, pp. 104–121.

[13]Siu, C. C., and Bert, C. W., "Sinusoidal Response of Composite-Material Plates with Material Damping," *Journal of Engineering for Industry*, Vol. 96, No. 2, 1974, pp. 603–610.

[14]Suarez, S. A., Gibson, R. F., Sun, C. T., and Chaturvedi, S. K., "The Influence of Fiber Length and Fiber Orientation on Damping and Stiffness of Polymer Composite Materials," *Experimental Mechanics*, Vol. 26, No. 2, 1986, pp. 175–184.

[15]Saravanos, D. A., and Chamis, C. C., "Computational Simulation of Structural Composite Damping," *Journal of Reinforced Plastics and Composites*, Vol. 10, No. 3, 1991, pp. 256–278.

[16]Bert, C. W., "Research on Dynamic Behavior of Composite and Sandwich Plates—IV," *Shock and Vibration Digest*, Vol. 17, No. 11, 1985, pp. 3–15.

[17]Liao, D. X., Sung, C. K., and Thompson, B. S., "The Optimal Design of Symmetric Laminated Beams Considering Damping," *Journal of Composite Materials*, Vol. 20, No. 5, 1986, pp. 485–501.

[18]Hajela, P., and Shih, C. J., "Optimum Synthesis of Polymer

Matrix Composites for Improved Internal Material Damping Characteristics," *AIAA Journal*, Vol. 26, No. 4, 1988, pp. 504–506.

[19]Saravanos, D. A., and Chamis, C. C., "Tailoring of Composite Links for Optimal Damped Elasto-Dynamic Performance," *Advances in Design Automation*, edited by B. Ravani, DE-Vol. 19-3, American Society of Mechanical Engineers, New York, 1989, pp. 151–159.

[20]Saravanos, D. A., and Chamis, C. C., "A Methodology for Optimizing Structural Composite Damping," *Journal of Polymer Composites*, Vol. 11, No. 6, 1990, pp. 328–336.

[21]Murthy, P. L. N., and Chamis, C. C., "ICAN: Integrated Composite Analyzer," *AIAA Paper 84-0974*, May 1984.

[22]Ginty, C. A., and Chamis, C. C., "Hygrothermomechanical Fiber Composite Fatigue: Computational Simulation," *Proceedings of the 33rd International SAMPE Symposium and Exhibition*, Vol. 33, Edited by G. Carillo et al., SAMPE, Covino, CA, 1988, pp. 1709–1720.

[23]Vanderplaats, G. N., "A Robust Feasible Directions Algorithm for Design Synthesis," *Proceedings of the 24th AIAA Structures, Structural Dynamics, and Materials Conference*, Pt. 1, 1983, pp. 392–399.